Appl Phys A (2012) 109:685–691
DOI 10.1007/s00339-012-7101-5

Applied Physics A
Materials Science & Processing

Fiber average size and distribution dependence on the electrospinning parameters of poly(vinylidene fluoride–trifluoroethylene) membranes for biomedical applications

V. Sencadas · C. Ribeiro · J. Nunes-Pereira · V. Correia · S. Lanceros-Méndez

Received: 23 March 2012 / Accepted: 3 August 2012 / Published online: 17 August 2012

Abstract Poly(vinylidene fluoride–trifluoroethylene), P(VDF–TrFE), electrospun membranes were obtained from a mixture of dimethylformamide (DMF) and methylethylketone (MEK) solvents. The inclusion of MEK to the solvent system promotes a faster solvent evaporation allowing complete polymer crystallization in the jet traveling between the tip and the grounded collector. The main electrospinning processing parameters were systematically changed to study their influence on fiber dimensions and distribution. Applied voltage and inner needle diameter do not have a large influence on the electrospun fiber average diameter but do on the fiber diameter distribution. On the other hand, increasing the distance between the needle tip and the collector gives origin to fibers with larger average diameter. Independently of the processing conditions, all membranes are produced in the electroactive phase of the polymer. Further, MC-3T3-E1 cell adhesion is not inhibited by the fiber membrane preparation, showing their potential use for biomedical applications.

Keywords Electroactive membranes · Electrospinning · Poly(vinylidene fluoride–trifluoroethylene) (P(VDF–TrFE)) · Tissue and biomedical engineering

V. Sencadas (✉) · C. Ribeiro · J. Nunes-Pereira · V. Correia · S. Lanceros-Méndez
Centro/Departamento de Física, Universidade do Minho, Campus de Gualtar, 4710-057 Braga, Portugal
e-mail: vsencadas@fisica.uminho.pt

V. Sencadas
Escola Superior de Tecnologia, Instituto Politécnico do Cávado e do Ave, Campus do IPCA, 4750-810 Barcelos, Portugal

V. Sencadas · C. Ribeiro · V. Correia · S. Lanceros-Méndez
International Iberian Nanotechnology Laboratory—INL, Avenida Mestre José Veiga s/n, 4715-330 Braga, Portugal

1 Introduction

There are a variety of processing techniques used to process micro- and nanofibers, such as drawing, template synthesis, wet spinning or phase separation. Most of these methods show important disadvantages as some processes are not scalable, are specific for a few number of polymers or there is no control over the fiber diameter or orientation [1]. Electrospinning has been demonstrated to be a unique method for the processing of sub-micron or even nanofibers from a polymer melt or solution, suitable for a broad set of polymer materials [1]. Electrospun fibers are intensively investigated due to their biomedical and tissue engineering applications (scaffolds, membranes, sutures, controlled release systems, etc.) [2] and for energy harvesting devices [3], among others.

Poly(vinylidene fluoride), PVDF, and poly(vinylidene fluoride–trifluoroethylene), P(VDF–TrFE), copolymers have attracted scientific and technological interest due to their chemical resistance, good mechanical properties and excellent electroactive properties [4–6]. P(VDF–TrFE) has a unique ferroelectric–paraelectric (FE–PE) phase transition within polymer materials. This FE–PE phase transition occurs in the bulk material at temperatures above room temperature and below the melting temperature ($T_c < T_m$). Further, the material shows a large electromechanical coupling coefficient [4, 7]. The crystalline structure of the ferroelectric phase consists in packed polymer chains in an *all-trans* planar zigzag configuration, with the dipolar moments parallel to the *b*-axis [4]. Above T_c, the paraelectric crystalline structure is hexagonal, consisting in a statistical configuration of TT, TG and TG′ rotational isomers [8]. The Curie temperature is highly dependent upon VDF content, but other factors also affect the ferroelectric transition temperature, such as electrical poling, heat treatment and processing history [6, 9, 10].

New and challenging research fields are emerging based on the application of piezoelectric materials such as energy harvesting [11] and biomedical application taking advantage of electroactive scaffolds [2, 12–15]. In these cases, piezoelectric nanofiber webs can show large advantages with respect to conventional thin films due to the larger surface to volume ratios and, therefore, large interaction areas. Some systematic works have been performed in PVDF in order to tailor electroactive phase content, fiber dimension and membrane porosity and morphology [16, 17], but just a few works are found concerning electrospinning of P(VDF–TrFE) copolymer, which shows the advantage of being able to be directly processed in the electroactive phase. Mandal et al. processed P(VDF–TrFE) oriented electrospun nanofibers by polymer dissolution in butan-2-one, showing that oriented fibers without beads or other defects can be obtained by using a drum collector with a rotational speed of 1000 rpm [3]. Electrospun scaffolds were also obtained by dissolution of P(VDF–TrFE) in methylethylketone (MEK) for a polymer concentration of 12–18 % for tissue engineering applications [18].

Random and aligned P(VDF–TrFE) nanofibers were also obtained from dissolution of the polymer in MEK with average fiber diameters of 3.22 ± 0.20 µm for randomly oriented fibers and 0.75 ± 0.08 µm for aligned fibers [19]. P(VDF–TrFE) membranes have also been obtained from dimethylformamide/acetone solvent mixtures [20]. The obtained materials show lower dielectric constant piezoelectricity than P(VDF–TrFE) films.

Despite these previous investigations and the large application potential of these materials, there is a lack of a systematic study of how the processing parameters influence the membrane fiber dimensions, which is one of the key features for tailoring membranes for specific applications. In the present work a novel route to process P(VDF–TrFE) by electrospinning was developed and a systematic study of the influence of the main electrospinning parameters such as applied voltage, needle inner diameter and solution flow rate on fiber morphology and distribution is presented. The suitability of the developed membranes for biomedical applications is proven by cell viability studies with osteoblast-like MC3T3-E1 cells.

2 Experimental

2.1 Materials

Poly(vinylidene fluoride–trifluoroethylene), P(VDF–TrFE), 70/30 was purchased from Solvay (Belgium) and dissolved in a mixture of solvents *N*,*N*-dimethylformamide (DMF, from Merck) and methylethylketone (MEK, from Panreac) (3.5/6.5 vol/vol) to achieve a polymer concentration of 15 wt% in the final solution. The polymer was dissolved at room temperature with the help of a magnetic stirrer until complete polymer dissolution.

2.2 Electrospinning

The polymer solution was placed in a commercial plastic syringe (10 ml) fitted with a steel needle with 500-µm inner diameter. Electrospinning was conducted in the range between 15 and 35 kV with a high-voltage power supply from Glassman (model PS/FC30P04). A syringe pump (from Syringepump) was used to feed the polymer solutions into the needle tip at a rate between 0.2 and 4 $\mathrm{ml\,h^{-1}}$. The electrospun fibers were collected in grounded collecting plates (random fibers) placed at a distance between 10 and 20 cm from the needle.

2.3 Characterization

Electrospun fibers were coated with a thin gold layer using a sputter coater (Polaron, model SC502) and their morphology was analyzed using a scanning electron microscope (SEM, Cambridge, Leica) with an accelerating voltage of 15 kV. The nanofiber average diameter and distribution were calculated over approximately 40 fibers using the SEM images at 2000× magnification and the Image J software.

Infrared measurements (Fourier transform infrared spectroscopy) were performed at room temperature with a Perkin-Elmer Spectrum 100 apparatus in ATR mode from 4000 to 650 $\mathrm{cm^{-1}}$. FTIR spectra were collected after 32 scans with a resolution of 4 $\mathrm{cm^{-1}}$.

The thermal behavior of the electrospun fiber mats was analyzed by differential scanning calorimetry (DSC) with a Pyris (Perkin-Elmer) apparatus. The samples were cut into small pieces from the middle region of the electrospun membranes, placed into 50-µl aluminum pans and heated to between 30 and 220 °C at a heating rate of 10 $\mathrm{°C\,min^{-1}}$. All experiments were performed under a nitrogen purge.

For cell culture, circular P(VDF–TrFE) nanofiber membranes with 13-mm diameter were prepared. For sterilization purposes, the nanofibers were immersed in 70 % ethanol for 30 min several times. Then, the membranes were washed five times for 5 min with phosphate-buffered saline (PBS), followed by three times with culture medium to eliminate any residual ethanol.

MC3T3-E1 cells (Riken cell bank, Japan) were cultivated in Dulbecco's modified Eagle's medium (DMEM) 1 g/L glucose (Gibco) containing 10 % fetal bovine serum (FBS) (Fisher) and 1 % penicillin/streptomycin (P/S).

For the study of cell viability, the osteoblast-like cells were seeded at a cell density of 3×10^4 cells/well for 2 days in 24-well TC plates containing the P(VDF–TrFE) fiber membranes. For the quantification of cell viability, MTT assay (Sigma-Aldrich) was carried out.

3 Results and discussion

Recent papers indicate that electrospinning of poly(vinylidene fluoride–trifluoroethylene) (PVDF–TrFE) can be performed from polymer dissolution in ethylmethylketone [18, 19]. Complete dissolution of the polymer in such solvent is difficult to achieve. Thus, P(VDF–TrFE) was electrospun at room temperature after complete dissolution in dimethylformamide (DMF), one of the most used solvents for PVDF and PVDF-related polymers. The polymer concentration in the solution was varied from 5 up to 20 % (w/v). The samples obtained in such conditions, independently of the needle inner diameter, distance from the tip to the collector, applied voltage or flow rate, presented a high concentration of beads (Fig. 1).

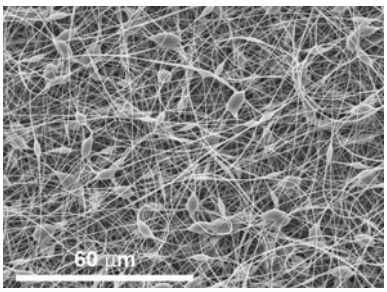

Fig. 1 P(VDF–TrFE) electrospun membrane obtained at 15/85 (15 % P(VDF–TrFE) + 85 % DMF by w/w) at a traveling distance of 20 cm, needle inner diameter of 0.5 mm, flow rate of 0.5 mL h^{-1} and applied voltage of 25 kV

Bead formation is one of the most common types of defect found in the processing of electrospun fibers [21] and occurs primarily as a result of the instability of the jet. These defects are typically related to the slow evaporation rate of the solvent during the traveling from the tip to the collector, due to the high DMF boiling point (153 °C, Table 1) [13].

In order to obtain well-formed fibers and samples without beads, a mixture of DMF and MEK solvents was used to dissolve the P(VDF–TrFE) polymer. These solvents were used due to their thermal and electrical properties: DMF (Table 1) shows a high dielectric constant, being one of the most used solvents for P(VDF–TrFE). It has, on the other hand, a quite high boiling point (Table 1). MEK has lower dielectric constant when compared to DMF but its lower boiling point allows faster polymer crystallization (Table 1).

The main electrospinning parameters were then varied in order to evaluate their influence on fiber size and size distribution. The influence of the applied voltage was investigated by keeping constant the value of the inner needle diameter at 0.5 mm, a flow rate of 0.5 ml h^{-1} and the traveling distance from the needle to the ground static collector of 20 cm. The morphology of the obtained samples is represented in Fig. 2. A histogram (Figs. 2c and 2d) of the fiber diameter distribution was determined from the SEM images and fiber average size and standard deviation were obtained.

Table 1 Physical and thermal properties of the solvents used in this work. Data collected from the material datasheets supplied by the manufacturers

Solvent	Melting point (°C)	Boiling point (°C)	Dipole moment (Debye)	Dielectric constant	Density (g/cm^3)
DMF	−61	153	382	38.2	0.944
MEK	−85	80	2.78	18.2	0.805

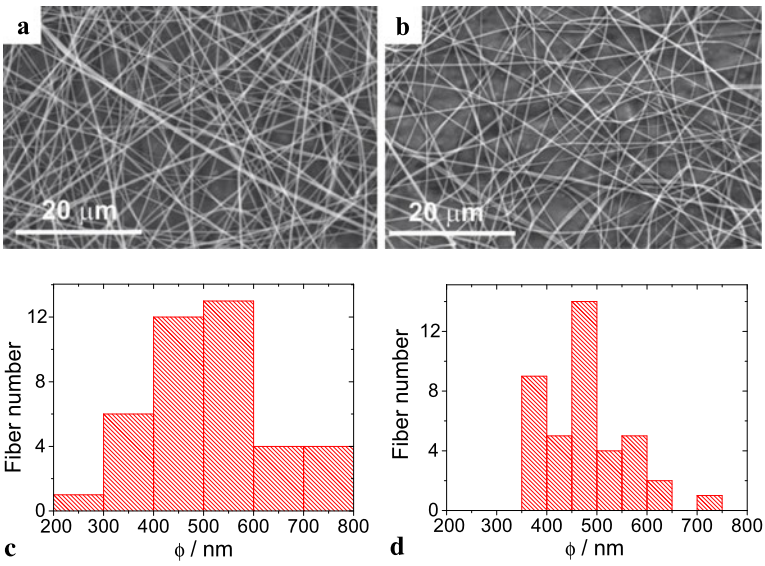

Fig. 2 P(VDF–TrFE) electrospun membrane obtained at 15/85 (15 % PVDF–TrFE + 85 % solvent blend) at a traveling distance of 20 cm, needle inner diameter of 0.5 mm, flow rate of 0.5 mL h^{-1} and applied voltages of 15 kV (**a** and **c**) and 35 kV (**b** and **d**)

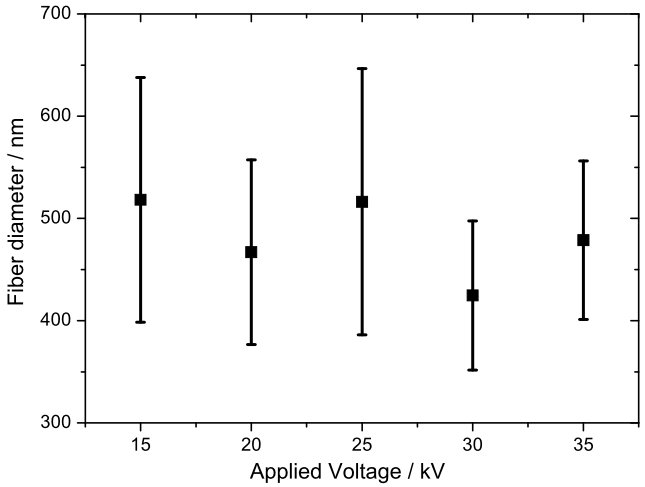

Fig. 3 Influence of applied electric field on the mean diameter of the electrospun P(VDF–TrFE) fibers. The flow rate was 0.5 mL h^{-1}, needle inner diameter of 0.5 mm and the distance between the tip and the collector of 20 cm

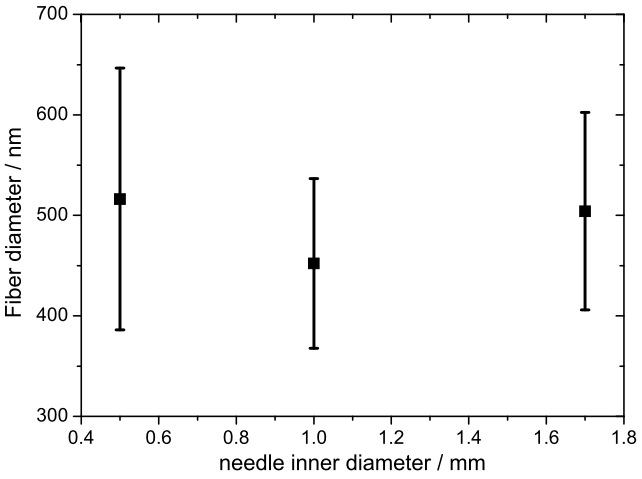

Fig. 4 Influence of needle inner diameter on the mean diameter of the electrospun P(VDF–TrFE) fibers. The flow rate was 0.5 mL h^{-1}, applied voltage of 25 kV and the distance between the needle and the collector of 20 cm

Figure 2 shows that the membranes obtained from a mixture of DMF and MEK can be electrospun without bead formation, with a smooth surface and randomly distributed fibers.

The mean diameter of the P(VDF–TrFE) fibers ranges between a maximum of 518 ± 119 nm and a minimum of 424 ± 72 nm for applied voltages of 15 and 30 kV, respectively (Fig. 3). Small variations are obtained but a trend to decreasing fiber diameter with increasing field can be identified due to variations of the mass flow and jet dynamics [1, 22].

The applied voltage is the drive of the electrospinning process. The formation of thin fibers is mainly achieved by the stretching and acceleration of the jets promoted by the high electric field [16, 23]. High applied voltage will result in higher charge density on the surface of the ejected jets; thus, the jet velocity increases and higher elongation forces are imposed to the jet. Consequently, it is generally reported that the diameter of the fibers becomes gradually smaller with increasing applied voltage [24–27]. On the other hand, as observed in the present experiments and also in other cases reported in the literature, this result is not general since changes in the applied voltage also affect other processing parameters such as traveling time of the jet, which has the opposite effect on the fiber diameter [28]. Further, increasing applied voltage often enhances jet instability, which results in a broader distribution of the fiber diameter [2, 16, 25]. In the present work, the variation of the fiber diameter (larger for lower voltages) and average size distribution (larger for lower voltages) with applied electric field is quite modest (Fig. 3), this parameter being not particularly relevant for the preparation of the electrospun mats.

Needle inner diameter can also play an important role in the electrospun fiber size and distribution. In this way, needles with different inner diameters were tested (Fig. 4).

It has been reported that smaller internal diameters reduce the clogging as well as prevent the formation of beads on electrospun fibers and that this effect can be attributed to a lower exposure of the solution to the atmosphere during electrospinning [29].

For P(VDF–TrFE) (Fig. 4) it is found that a decrease of the needle inner diameter has no strong influence on the fiber mean diameter, but results in a broader distribution of the fiber sizes. When the size of the droplet at the tip decreases, such as is the case of the smaller needle inner diameters, the surface tension of the droplet increases and, for the same applied voltage, a larger Coulomb force is required to cause the jet initiation. As a result, the acceleration of the jet decreases, allowing more time for the solution to be stretched and elongated before it is collected in the ground metallic collector [1]. This leads to a broader distribution of the fiber diameter for small internal needle tips (Fig. 4).

The influence of the solution flow rate on fiber size and distribution was characterized by keeping constant the applied voltage (25 kV) and needle inner diameter (0.5 mm) (Fig. 5).

Feed rate will determine the amount of polymer solution available for electrospinning for a given voltage [1]. It is expected that increasing feed rates leads to an increase of the fiber diameter or to the presence of beads due to the larger volume of solution drawn away from the needle. The increase of drawn volume from the needle tip will promote an increase of the evaporation time of the solvent and therefore a larger polymer crystallization time, giving origin to larger fiber diameters and a broader size distribution. For

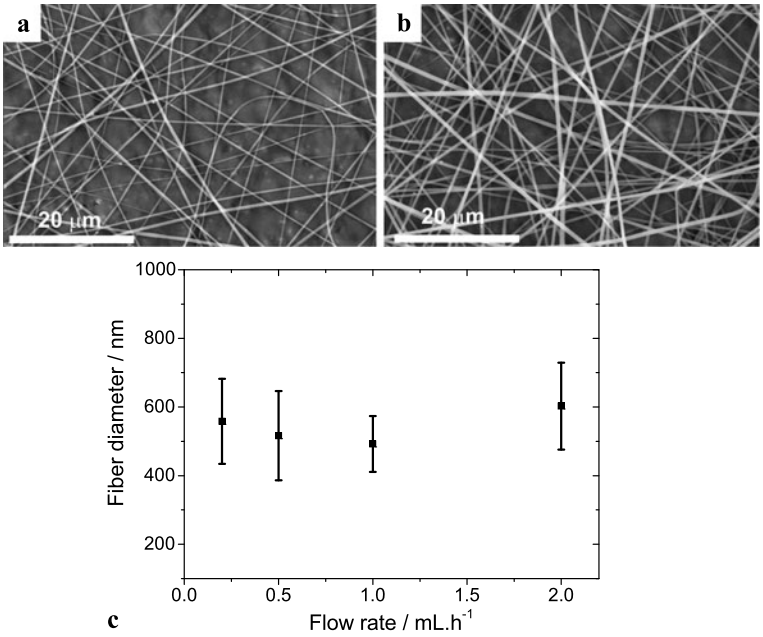

Fig. 5 Influence of flow rate on the mean diameter of the electrospun P(VDF–TrFE) fibers. The needle inner diameter was 0.5 mm, applied voltage of 25 kV and the distance between the tip and the collector of 20 cm: (**a**) sample obtained at 1 mL h^{-1}, (**b**) sample obtained at 2 mL h^{-1} and (**c**) fiber average size and distribution dependence on flow rate

the range of feed rates tested, no significant dependence of the fiber diameter was observed (Fig. 5). Moreover, the optimum feed rate to stabilize the Taylor cone is 1 mL h^{-1} for the applied voltage of 25 kV and the traveling distance of 20 cm. Smaller diameters for the fibers were obtained also when compared to lower flow rates, meaning that under these conditions, the jet acceleration decreases allowing more time for the solution to be stretched and elongated before it was collected.

Flight time and electric field strength affect the electrospinning process and the resulting fiber morphology. Varying the distance between the needle tip and the ground collector will have a direct influence on both the flight time and the electric field strength. The influence of the tip to collector distance on the nanofiber diameter and distribution is shown in Fig. 6.

In order to promote the formation of independent fibers, most of the solvent evaporation must occur during the traveling distance between the tip and the metallic ground collector. When the distance is reduced, the jet will have a shorter distance to travel and consequently the time available for solvent evaporation decreases. Moreover, the electric field strength increases at the same time and this will increase the acceleration of the jet to the collector. Figure 6 shows that well-formed nanofibers were obtained for needle–collector distances larger than 10 cm and that the fiber diameter and distribution increase with increasing distance up to 20 cm. A decrease in the tip to ground collector distance has a similar effect to the increase of the applied voltage, leading to smaller fiber diameters.

The crystalline phase present in the electrospun P(VDF–TrFE) membranes was identified by differential scanning

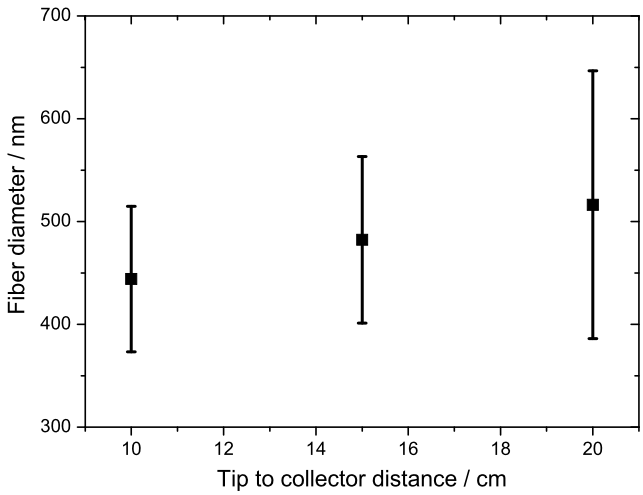

Fig. 6 Influence of the distance between the needle tip and the ground metallic collector on the fiber mean diameter for the electrospun P(VDF-TrFe) membrane. The tip inner diameter was 0.5 mm, applied voltage of 25 kV and flow rate of 0.5 mL h^{-1}

calorimetry (DSC) and Fourier transform infrared (FTIR) spectroscopy.

In the DSC thermograms (Fig. 7a) two peaks are observed: the one that occurs at the lower temperature corresponds to the ferroelectric–paraelectric transition (FE–PE, Curie transition) with maximum at ~117 °C. The higher DSC endotherm corresponds to the melting of the polymer and it is located at ~145 °C. It can be observed that the electrospinning process does not affect polymer melting temperature but a small increase in the FE–PE transition temperature was observed for samples processed with applied voltages higher than 25 kV, which is possibly related to the elec-

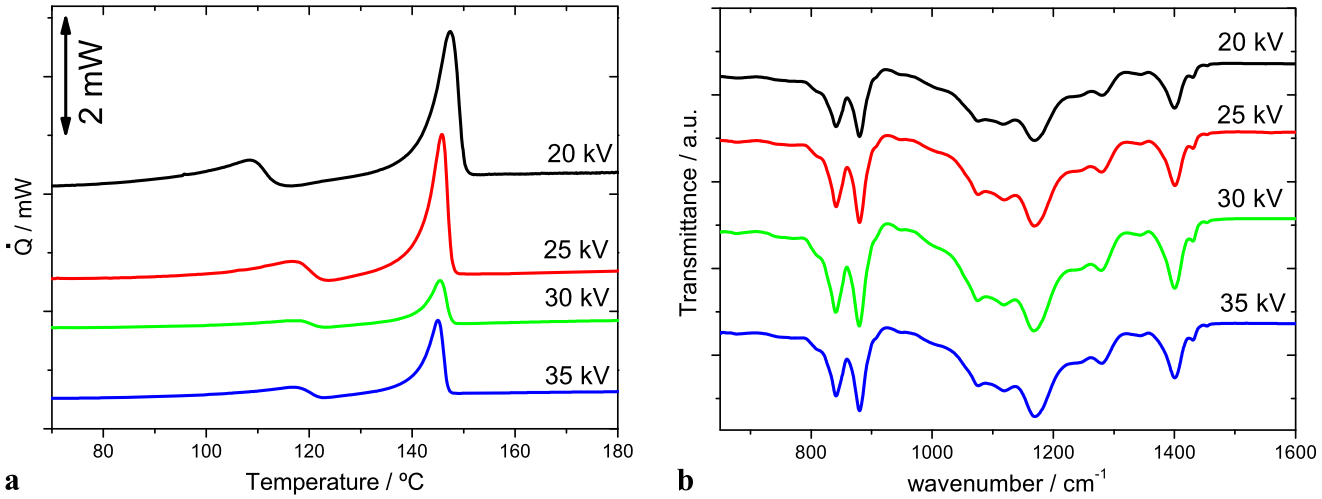

Fig. 7 (**a**) DSC results for the P(VDF–TrFE) electrospun membranes and (**b**) infrared spectra for the samples prepared with tip inner diameter of 0.5 mm, applied voltage of 25 kV, flow rate of 0.5 mL h^{-1} and the distance between tip and collector of 20 cm

tric poling effect promoted by the electrospinning technique that tends to orient the polymer dipoles in the direction of the applied electric field [3].

P(VDF–TrFE) is a semicrystalline polymer that crystallizes in the electroactive phase. FTIR spectra of electrospun samples show that the crystallization of the polymer occurs in the ferroelectric phase (Fig. 7b) due to the presence of the absorption band at 840 cm^{-1}, characteristic of this phase, and the absence of absorption modes of the α-phase of PVDF (that occur at 855, 795 and 766 cm^{-1}) or of γ-phase (833, 812 and 776 cm^{-1}) [16].

P(VDF–TrFE) is therefore obtained by electrospinning in the electroactive phase, showing a large potential for biomedical and tissue engineering applications, especially for bone repair [30], nerve guidance [31, 32] or even cochlea reconstruction [33].

The electrospinning process uses many times toxic solvents that could eventually prevent the use of the membranes in biomedical applications. MTT tests were used to characterize proliferation and viability of cells on P(VDF–TrFE) as-spun fiber membranes throughout 2 days of culture. The absorbance (A) was measured at 570 nm for all the samples (Fig. 8). It was observed that electrospun fiber mats prepared under the above-described method and conditions do not inhibit the adhesion of cells for the 2 days.

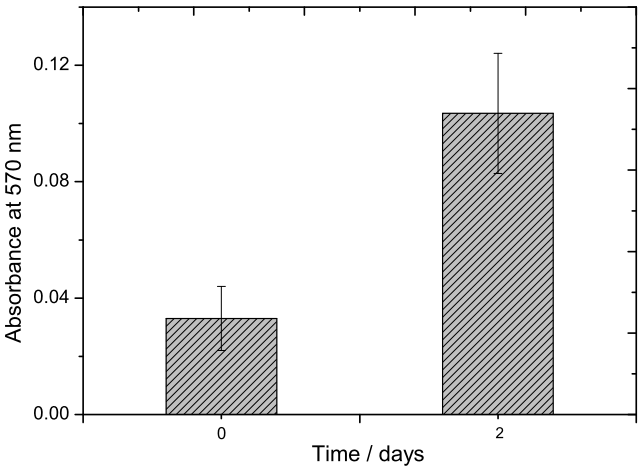

Fig. 8 MTT absorbance for cells seeded for 0 and 2 days on PVDF–TrFE nanofibers. Values are mean ± SD

4 Conclusions

Poly(vinylidene fluoride-trifluoroethylene) electrospun fiber mats with fiber diameters in the range 400 to 500 nm have been obtained from a DMF and MEK solvent solution. The inclusion of MEK to the solvent system promotes a faster solvent evaporation and allows complete polymer crystallization in the jet traveling between the tip and the grounded collector, avoiding the presence of beads in the fiber mats.

The influence of applied voltage, flow rate and needle inner diameter on the average fiber diameter and fiber diameter distribution was investigated. Whereas applied voltage and needle diameter have no strong influence on fiber diameter, a larger dependence is obtained by varying the flow rate. Also, the fiber diameter increases by increasing the distance from the tip to the ground collector.

The polymer crystalline phase and its thermal features are not affected by the processing conditions. MC-3T3-E1 cell adhesion was not inhibited by the fiber mat preparation, indicating the suitability of the material for biomedical applications.

Acknowledgements This work is funded by FEDER funds through the 'Programa Operacional Factores de Competitividade—COMPETE' and by national funds arranged by FCT—Fundação para a Ciência e a Tecnologia, project references NANO/NMed-SD/0156/2007, PTDC/CTM/73030/2006 and PTDC/CTM/69316/2006. The authors also acknowledge support from the COST Action MP1003, 2010 'European Scientific Network for Artificial Muscles'. V.S., V.C. and J.N.P. thank the FCT for the SFRH/BPD/63148/2009, SFRH/BD/48708/2008 and SFRH/BD/66930/2009 grants, respectively. C.R. thanks the IINL for financial support via a Ph.D. studentship.

References

1. S. Ramakrishna, K. Fujihara, W.-E. Teo, T.-C. Lim, Z. Ma, *An Introduction to Electrospinning and Nanofibers* (World Scientific, Singapore, 2005)
2. C. Ribeiro, V. Sencadas, C.M. Costa, J. Gómez Ribelles, S. Lanceros-Méndez, Sci. Technol. Adv. Mater. **12**, 015001 (2011)
3. D. Mandal, S. Yoon, K.J. Kim, Macromol. Rapid Commun. **32**, 831 (2011)
4. A.J. Lovinger, Science **220**, 1115 (1983)
5. H.S. Nalwa, *Ferroelectric Polymers: Chemistry, Physics, and Applications* (Dekker, New York, 1995)
6. V. Sencadas, S. Lanceros-Méndez, J.F. Mano, J. Non-Cryst. Solids **352**, 5376 (2006)
7. L.F. Brown, IEEE Trans. Ultrason. Ferroelectr. Freq. Control **47**, 1377 (2000)
8. V. Sencadas, S. Lanceros-Méndez, J.F. Mano, Solid State Commun. **129**, 5 (2004)
9. R. Tanaka, K. Tashiro, M. Kobayashi, Polymer **40**, 3855 (1999)
10. K.K. Jin, K.G. Bum, Polymer **38**, 4881 (1997)
11. Z.L. Wang, J. Song, Science **312**, 242 (2006)
12. A. Ferreira, J. Silva, V. Sencadas, J.L.G. Ribelles, S. Lanceros-Méndez, Macromol. Mater. Eng. **295**, 523 (2010)
13. R. Magalhães, N. Durães, M. Silva, J. Silva, V. Sencadas, G. Botelho, J.L. Gómez Ribelles, S. Lanceros-Méndez, Soft Mater. **9**, 1 (2010)
14. A. Ferreira, J. Silva, V. Sencadas, J.L. Gómez-Ribelles, S. Lanceros-Méndez, Mater. Res. Soc. Symp. Proc. **1312**, 125–130 (2011)
15. A. California, V.F. Cardoso, C.M. Costa, V. Sencadas, G. Botelho, J.L. Gómez-Ribelles, S. Lanceros-Mendez, Eur. Polym. J. **47**, 2442 (2011)
16. C. Ribeiro, V. Sencadas, J.L.G. Ribelles, S. Lanceros-Méndez, Soft Mater. **8**, 274 (2010)
17. W. Liu, X. Cheng, X. Fu, C. Stefanini, P. Dario, Microelectron. Eng. **88**, 2251 (2011)
18. N. Weber, Y.S. Lee, S. Shanmugasundaram, M. Jaffe, T.L. Arinzeh, Acta Biomater. **6**, 3550 (2010)
19. Y.-S. Lee, G. Collins, T.L. Arinzeh, Acta Biomater. **7**, 3877 (2011)
20. F. He, M. Sarkar, S. Lau, J. Fan, L.H. Chan, Polym. Test. **30**, 436 (2011)
21. A.L. Andrady, *Science and Technology of Polymer Nanofibers* (Wiley, New York, 2008)
22. S.-Y. Gu, J. Ren, Macromol. Mater. Eng. **290**, 1097 (2005)
23. X.-H. Qin, Y.-Q. Wan, J.-H. He, J. Zhang, J.-Y. Yu, S.-Y. Wang, Polymer **45**, 6409 (2004)
24. S. Zhao, X. Wu, L. Wang, Y. Huang, J. Appl. Polym. Sci. **91**, 242 (2004)
25. K. Gao, X. Hu, C. Dai, T. Yi, Mater. Sci. Eng. B **131**, 100 (2006)
26. M.M. Demir, I. Yilgor, E. Yilgor, B. Erman, Polymer **43**, 3303 (2002)
27. S. Megelski, J.S. Stephens, D.B. Chase, J.F. Rabolt, Macromolecules **35**, 8456 (2002)
28. V. Sencadas, D.M. Correia, A. Areias, G. Botelho, A.M. Fonseca, I.C. Neves, J.L. Gómez-Ribelles, S. Lanceros-Méndez, Carbohydr. Polym. **87**, 1295 (2012)
29. X.M. Mo, C.Y. Xu, M. Kotaki, S. Ramakrishna, Biomaterials **25**, 1883 (2004)
30. R. Gimenes, M.A. Zaghete, M. Bertolini, J.A. Varela, L.O. Coelho, N.F. Silva Jr., SPIE Proc. **5385**, 539–547 (2004)
31. E.G. Fine, R.F. Valentini, R. Bellamkonda, P. Aebischer, Biomaterials **12**, 775 (1991)
32. Y.-S. Lee, T.L. Arinzeh, Polymers **3**, 413 (2011)
33. H. Shintaku, T. Tateno, N. Tsuchioka, H. Tanujaya, T. Nakagawa, J. Ito, S. Kawano, J. Biomech. Sci. Eng. **5**, 229 (2010)